International Conference on Control, Automation and Systems 2008
Oct. 14-17, 2008 in COEX, Seoul, Korea

Autonomous Flight Control System Design for a Blended Wing Body

D.Jin Lee[1] , Byoung-Mun Min[2], Min-Jea Tahk[2], Hyochoong Bang[1], D.H Shim[2]

[1] Division of Aerospace Engineering, School of Mechanical, Aerospace & Systems Engineering, KAIST, Daejeon, Korea
(Tel : +82-42-869-{5779, 3722}; E-mail: {djlee, hcbang}@ascl.kaist.ac.kr)

[2] Division of Aerospace Engineering, School of Mechanical, Aerospace & Systems Engineering, KAIST, Daejeon, Korea
(Tel : +82-42-869-{5758, 3718, 3724}; E-mail: {bmmin, mjtahk, hcshim}@fdcl.kaist.ac.kr)

Abstract: A Blended Wing Body (BWB) UAV has several aerodynamic advantages of lower wetted area to volume ratio and lower interference drag as compared to conventional type UAV. This paper is focused on the design of the autonomous flight control system for a BWB UAV. An onboard control system is developed by using a powerful computer, navigation sensors and communication modem. The autopilot of the BWB UAV is constructed based on the stability analysis using the linearized model at trim condition. We propose a simple control allocation scheme and evaluate its performance through nonlinear simulation. Furthermore, flight test is performed using the designed autopilot and satisfactory performance is obtained in autonomous flight.

Keywords: Blended Wing Body UAV, Autopilot, Nonlinear simulation, Control allocation, Stability analysis

1. INTRODUCTION

A BWB type aircraft is a revolutionary conceptual change from the conventional aircraft and sometimes referred to a 'flying wing' due to its configuration of the integrated wing and fuselage. Actually, the BWB configuration has been proposed to improve the economic efficiency of future air transportation [1, 2]. The BWB configuration increases the maximum lift-to-drag ratio to about 20% and shows lower stall speed without flap over conventional one. Nevertheless, these significant benefits, stability and control problem are still remained as the main drawback of BWB configuration [5]. In the aspect of stability, aerodynamic center is very closely located to center of gravity(CG) or is located ahead of the CG. Also, BWB UAV has low directional stability and adverse yaw characteristics during rolling maneuver [2]. Moreover, since the two control surfaces simultaneously generate the longitudinal and the lateral-directional motions, control allocation scheme is necessarily implied to flight control system of BWB UAV.

In this paper, a detailed dynamic model of the BWB UAV is constructed and then the flight performance and stability are analyzed. After designing the autopilot with the dynamic model applying a simple control allocation scheme, we evaluate its control performance through nonlinear simulation.

Consequently, we integrate the BWB UAV platform with onboard computer, navigation sensors, and communication modem and perform the real flight test.

2. SYSTEM OVERVIEW

To demonstrate the autonomous flight, it is needed to integrate the BWB UAV platform with the suitable hardware and software so that the vehicle can perform the desired autonomous maneuvers. Since the limit of the mass budget and mounting space, lighter instruments should be selected. The flight control computer (FCC) acquires its attitude data from the sensors attached to the vehicle such as GPS, attitude heading reference system (AHRS). By using common personal computer, GCS is constructed. Real time kernel is selected to operate the FCC.

2.1 BWB Model

To demonstrate the real flight test, a reliable vehicle platform is significant. In this paper, a small BWB model aircraft had been adopted for the ease of maintenance. The onboard computer is equipped on the center of the body. The detailed specification of this model is shown in the Fig. 1 and Table 1.

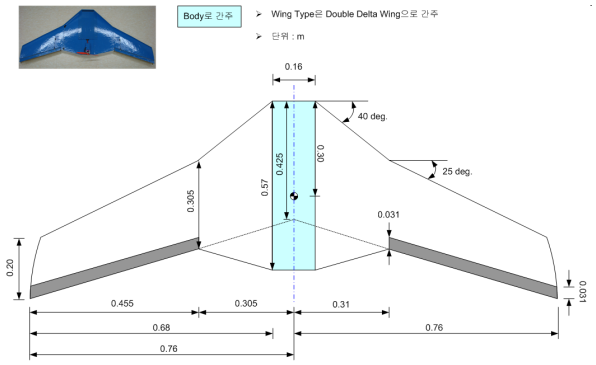

Fig. 1 BWB model

Table 1 Physical parameters of the BWB UAV.

Weight (kg)	empty	1.2	including battery and motor	
	total	2.5	including FCC and navigation sensors	
Moment of inertia (kg.m^2)	I_{xx}	0.1080	Wing span (m)	1.52
	I_{yy}	0.0423	Wing area (m^2)	0.554
	I_{zz}	0.1361	Mean aerodynamic Chord (m)	0.29

2.2 Flight Control Computer

The flight control computer plays an important role to control the attitude and the velocity of the vehicle on the basis of the data from each sensor. FCC is consists of CPU board and peripheral boards such as power board, data modem and so on. A PC/104 commercial on-board computer is selected due to small size, reliability, powerful CPU and extendibility.

2.3 Navigation Sensors

The strap-down inertial measurement unit (IMU) is usually applied to small UAV systems because they are more suitable for small size application than the mechanical platform IMU in terms of size and weight. The AHRS is used for measuring angular rates, linear accelerations, and attitudes of the vehicle. It uses three gyroscopes, three accelerometers, three magnetic sensors with internal power regulations, and signal processing electronics. The global positioning system is a satellite navigation system. More than two dozens of GPS satellites are orbiting the Earth and transmit radio signals which allow any GPS receiver near the planet to determine its location, speed and direction.

3. AUTOPILOT DESIGN

3.1 Modeling of the BWB UAV

The 6-DOF equations of motion of the BWB UAV can be represented as the same manner of conventional type aircraft under the assumption of the flat Earth and constant mass properties. The rotational and translational motion can be derived as follows;

$$\begin{aligned}
\dot{U} &= RV - QW - g_0 \sin\theta + F_x / m \\
\dot{V} &= -RU + PW + g_0 \sin\phi\cos\theta + F_y / m \\
\dot{W} &= QU + PV + g_0 \cos\phi\cos\theta + F_z / m
\end{aligned} \tag{1}$$

$$\begin{aligned}
\dot{P} &= (c_1 R + c_2 P)Q + c_3 L + c_4 N \\
\dot{Q} &= c_5 PR - c_6 (P^2 - R^2) + c_3 M \\
\dot{R} &= (c_8 P - c_2 R)Q + c_4 L + c_9 N
\end{aligned} \tag{2}$$

where the notation and the definition of c1 to c9 are referred to Ref. [7].

In general, aerodynamic coefficients are obtained from theoretical and experimental works such as CFD analysis, wind tunnel test, and flight test. In this paper, non-dimensional aerodynamic static and dynamic stability derivatives are calculated by using the software of 'Digital DATCOM'. 'Digital DATCOM' calculates static stability, high-lift and control device, and dynamic-derivative characteristics using the geometric data as shown in Fig. 1. It also offers a trim option that computes control deflections and aerodynamic data for vehicle trim at subsonic Mach numbers [8].

Fig. 2 and Fig. 3 show static stability and control derivatives that are calculated from 'Digital DATCOM'. For the BWB UAV considered in this research, only one pair of control surfaces as shown in Fig. 1 is taken a role as an elevon, i.e. right and left control surfaces are deflected in the same direction for pitch control and deflected in the opposite direction for roll control. In Fig. 3, we can find the fact that the effect of pitching moment is about 10 times larger than the effect of roll moment by deflection of the control surface. This phenomenon is related with the configuration that has the reduced kinematic damping in the pitching motion.

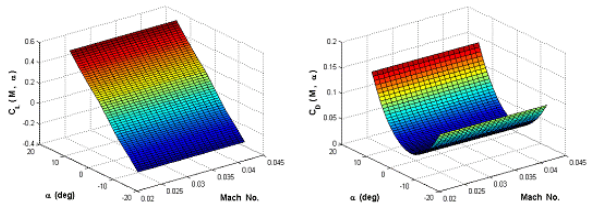

Fig. 2 Static Stability derivatives

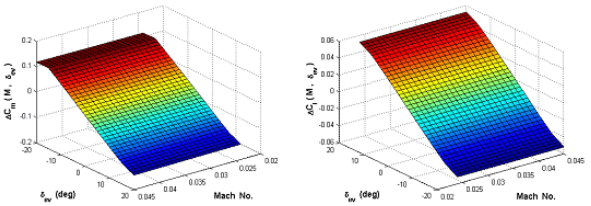

Fig. 3 Control derivatives

3.2 Flight Controller Design

A nonlinear simulation model is developed by using parameters obtained from the DATCOM. Since the derived model includes a complex nonlinear dynamics equation, it is required to linearize the system around a trim point to analyze the system stability and performance. We obtained a trim condition for the steady-state level flight at the altitude of 100m and the speed of 12m/s. The trim condition is listed in the Table 2. At this trim condition, a set of linear longitudinal and lateral dynamics is derived in state-space form as follows;

- *Longitudinal dynamics*

$$\begin{bmatrix} \dot{V}_T \\ \dot{\alpha} \\ \dot{\theta} \\ \dot{q} \\ \dot{h} \end{bmatrix} = \begin{bmatrix} -0.239 & 1.513 & -9.810 & 0.000 & 0.000 \\ -0.133 & -5.940 & 0.000 & 0.922 & 0.000 \\ 0.000 & 0.000 & 0.000 & 1.000 & 0.000 \\ 0.017 & -170.612 & 0.000 & -7.853 & 0.000 \\ 0.000 & -12.000 & 12.000 & 0.000 & 0.000 \end{bmatrix} \begin{bmatrix} V_T \\ \alpha \\ \theta \\ q \\ h \end{bmatrix} + \begin{bmatrix} 6.741 & -0.006 & -0.006 \\ -0.090 & -0.008 & -0.008 \\ 0.000 & 0.000 & 0.000 \\ 0.000 & -1.328 & -1.328 \\ 0.000 & 0.000 & 0.000 \end{bmatrix} \begin{bmatrix} \delta_{th} \\ \delta_{ev}^R \\ \delta_{ev}^L \end{bmatrix} \tag{3}$$

- *Lateral dynamics*

$$\begin{bmatrix} \dot{\beta} \\ \dot{\phi} \\ \dot{\psi} \\ \dot{p} \\ \dot{r} \end{bmatrix} = \begin{bmatrix} -0.072 & 0.807 & 0.000 & 0.159 & -0.987 \\ 0.000 & 0.000 & 0.000 & 1.000 & 0.161 \\ 0.000 & 0.000 & 0.000 & 0.000 & 1.013 \\ -115.511 & 0.000 & 0.000 & -10.254 & 1.445 \\ -15.179 & 0.000 & 0.000 & -0.023 & -0.233 \end{bmatrix} \begin{bmatrix} \beta \\ \phi \\ \psi \\ p \\ r \end{bmatrix} + \begin{bmatrix} 0.000 & 0.000 & 0.000 \\ 0.000 & 0.000 & 0.000 \\ 0.000 & 0.000 & 0.000 \\ 0.000 & -0.930 & 0.930 \\ 0.000 & -0.132 & 0.132 \end{bmatrix} \begin{bmatrix} \delta_{th} \\ \delta_{ev}^R \\ \delta_{ev}^L \end{bmatrix} \tag{4}$$

Table 2 Trim condition of the BWB UAV

Flight Condition		Trim State Value		Control Input for Trim Flight	
Speed (m/s)	12	Angle-Of-Attack (deg)	9.14	Throttle Level	0.15
Altitude (m)	100	Flight Path Angle (deg)	0.00	Elevon Deflection Angle (deg)	-2.54

In these linearized dynamic models, short period mode is fast and the damping ratio is comparatively small. Unfortunately, also it has an unstable dutch-roll mode, which may be caused by the fact that there is no appropriate control surface such as rudder in order to damp out yawing oscillation even though it has a sweep-back wing.

The autopilot for longitudinal and lateral-directional motions is designed by applying the classical approach referred to Ref. [7]. As shown in Fig. 4, longitudinal autopilot consists of speed controller and altitude hold controller that are integrated with the inner-loop controllers for pitch attitude stabilization and orientation.

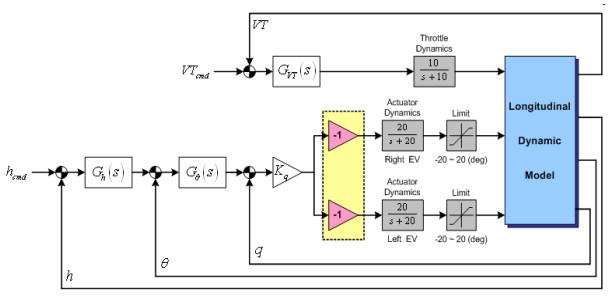

Fig. 4 Autopilot structure for longitudinal direction

Lateral-directional autopilot is focused on the control of heading orientation that is constituted with the inner-loop controller for roll stabilization and orientation as shown in Fig. 5.

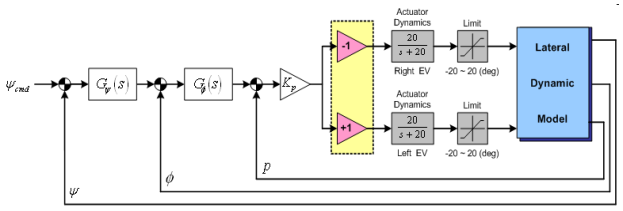

Fig. 5 Autopilot structure for lateral direction

The gains in the dotted-line box of Fig. 4 and Fig. 5 are for determining the direction of deflection of each elevon that describe the control allocation scheme. The designed controllers for autopilot of BWB UAV are summarized in Table 3. The bode diagrams of altitude hold and heading control loop represent that the designed autopilot system assures a sufficient gain margin and phase margin.

Table 3 Autopilot of the BWB UAV

Speed Control Loop	Altitude Hold Loop	Heading Orientation Loop
$G_{VT}(s)=\frac{0.4s+0.12}{s}$	$K_q=8.0$	$K_p=10.0$
	$G_\theta(s)=\frac{5.0s+2.5}{s}$	$G_\theta(s)=\frac{5.0s+1.2}{s}$
	$G_h(s)=\frac{0.05s+0.01}{s}$	$G_\psi(s)=2.5$

Since the motions of the BWB UAV are controlled by only one elevon control surface, control allocation technique is need to generate control signal to each control surface effectively in order to merge the longitudinal and lateral-directional autopilot. Although there are several researches related to applying control allocation scheme to control of BWB aircraft [5, 9], we distribute the control signals into right and left elevon using a simple distributor as shown in Fig. 6.

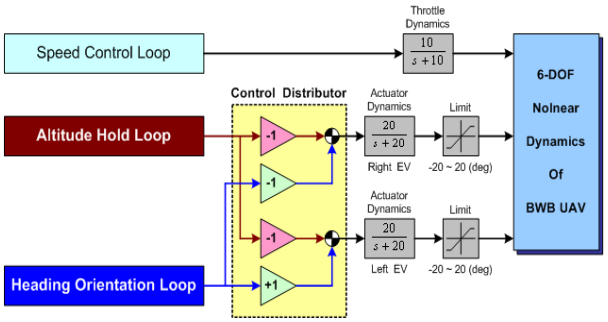

Fig. 6 Control distributor for autopilot of BWB UAV

Fig. 7 represents the control performance of the designed autopilot when the step input command of altitude and heading angle is simultaneously imposed. From the results, we can observe that the performance of heading orientation loop is poor compared to altitude hold loop. In fact, in order to improve this control performance, optimal control allocation should be designed and integrated into autopilot. The right and left elevons are actuated asymmetrically during the initial transient period to achieve the control objective.

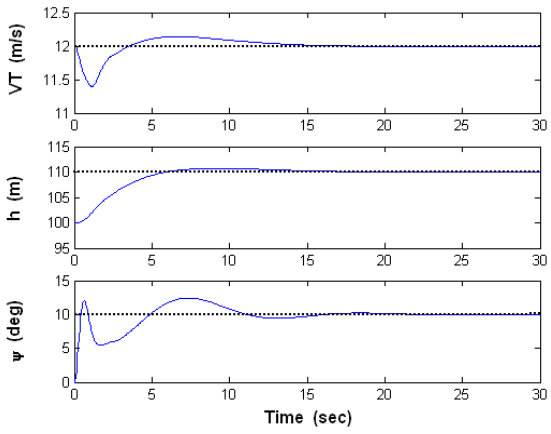

Fig. 7 Control performance of the autopilot

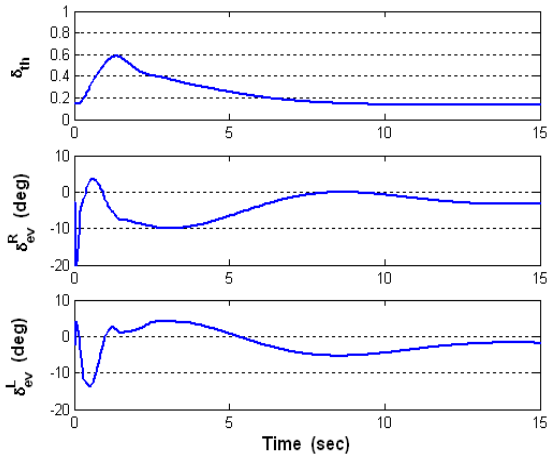

Fig. 8 Deflection of the control surface and throttle level

4. FLIGHT TEST

A series of flight tests have been performed using the developed BWB UAV. Fig. 9 shows the flight data on altitude channel during the vehicle is commanded to perform level flight at 100m above the ground. Fig. 10 shows the flight result of heading orientation during the vehicle is commanded to hold -100 deg from the north. From the flight data, we can observe that the designed autopilot control the BWB UAV satisfactory.

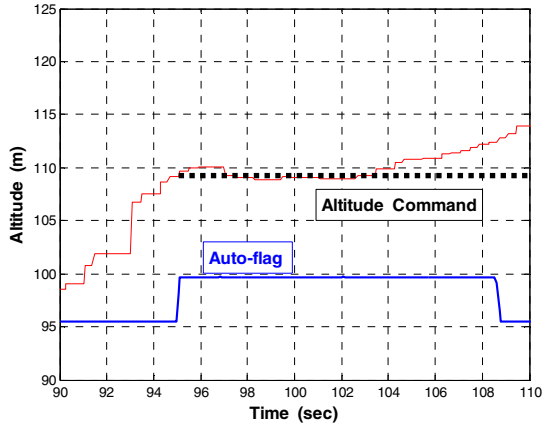

Fig. 9 Flight test result of altitude channel

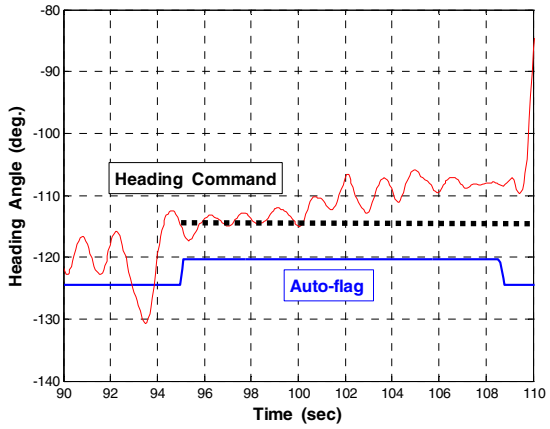

Fig. 10 Flight test result of heading channel

Fig. 11 represents the trajectory of vehicle during the waypoint navigation. Since the scale of the waypoint is relatively small, the overshoot may be occurred.

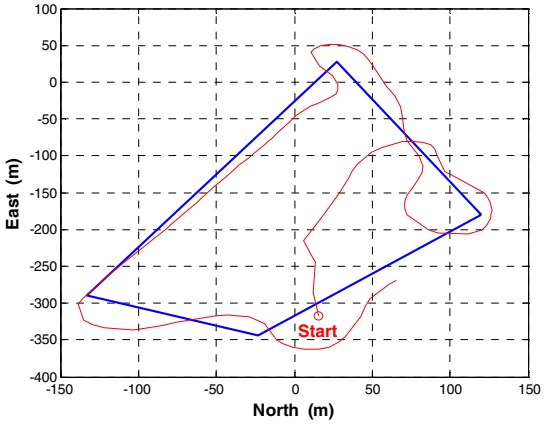

Fig. 11 2D trajectory of the BWB UAV

5. CONCLUSION

The BWB model platform is integrated with onboard computer and sensors to implement autonomous flight. The autopilot is designed with the linear model obtained from the nonlinear BWB model using the software of 'Digital DATCOM'. The linearized model provided the specific flying characteristics of BWB UAV, such as unstable dutch-roll mode. The autopilot for speed, altitude, heading control was evaluated through the nonlinear simulation. Furthermore, we performed real flight tests to verify the control performance of the developed autopilot system. Consequently, we obtained satisfactory flight data and applied the autopilot to waypoint navigation.

ACKNOWLEDGEMENTS

The authors gratefully acknowledge for financial support by Korea Ministry of Knowledge Economy.

REFERENCES

[1] Portsdam, M. A., Page, M. A., and Liebeck, R. H., "Blended Wing Body Analysis and Design," *AIAA Paper 97-2317*, 1997.

[2] Nickel, K. and Wohlfahrt, M., Tailless Aircraft in Theory and Practice, *AIAA Education Series*, 1994.

[3] Qin. N., Vavalle, A., Le Moigne, A., Laban, M., Hackett, K., and Weinerfelt, P., "Aerodynamic consideration of blended wing body aircraft," *Progress in Aerospace Science*, Vol. 40, pp. 321-343, 2004.

[4] Qin, N., Vavalle, A., and Le Moigne, A., "Spanwise Lift Distribution for Blended Wing Body Aircraft," *Journal of Aircraft*, Vol. 42, No. 2, pp. 356-365, Mach-April 2005.

[5] Jung, D. W. and Lowenberg, M. H., "Stability and Control Assessment of a Blended- Wing-Body

Airliner Configuration," *AIAA Atmospheric Flight Mechanics Conference and Exhibit*, San Francisco, California, Aug. 2005.

[6] Donlan, C. J., "An interim report on the stability and control of tailless airplanes," *NACA Report* No. 796, Aug. 1944.

[7] Stevens, B. L. and Lewis, F. L., “Aircraft Control and Simulation”, John Wiley & Sons, Inc., New York, 1992.

[8] The USAF Stability and Control DATCOM Volume 1, Users Manual, McDonnell Douglas Astronautics Company, April 1979.

[9] Buffington, J. M., "Tailless Aircraft Control Allocation," *AIAA Paper 97-3605*, 1997